Table IV. Angular Dependence of EPR Line Widths for $(RNH_3)_2CuBr_4$ Salts at 77 K

compds	ΔH_{pp}, Oe	compds	ΔH_{pp}, Oe
$(\beta\text{-alaH})_2CuBr_4$	$49 + 14\cos^2\theta$	$(PA)_2CuBr_4$[a]	$97 + 28\cos^2\theta$
$(EA)_2CuBr_4$[a]	$111 + 20\cos^2\theta$	$(PDA)CuBr_4$[a]	$118 + 20\cos^2\theta$

[a] Reference 9.

Conclusions

The salt $(\beta\text{-alaH})_2CuBr_4$ has been shown to be a two-dimensional system with strong ferromagnetic intralayer coupling. The value of $J/k = 21.2$ K obtained is comparable that for to other $(RNH_3)_2CuBr_4$ salts. The exchange interaction is very nearly Heisenberg in nature, with only a small orthorhombic anisotropy. The easy axis is normal to the layer. Consistent with results on other $(RNH_3)_2CuX_4$ systems, the magnetic data indicate that the $(\beta\text{-alaH})_2CuX_4$ salts switch from a predominant XY anisotropy in the chloride salt to a predominant Ising anisotropy in the bromide salt. This changeover is probably a direct result of the reduction of single-ion anisotropy for the bromide salt with respect to the chloride salt. The value of $g_\perp - g_\parallel$, which contributes toward an XY-like anisotropy, is reduced from 0.116 for $(\beta\text{-alaH})_2CuCl_4$ to 0.054 for $(\beta\text{-alaH})_2CuBr_4$.

It has been shown that the angular dependence of the EPR line widths can be accounted for by the contributions of the magnetic anisotropies to the relaxation processes. Thus, the EPR behavior of the $(RNH_3)_2CuBr_4$ salts can be accounted for by the same formalism as proposed by Soos et al.[1] for $(RNH_3)_2CuCl_4$ salts. In an examination of the trends in the spin anisotropies as determined by the EPR measurements (Table IV), it is observed that $R_A(Br) < {}^1/_2R_A(Cl)$. The d_x and d_y components of the antisymmetric exchange would be expected to lead to an Ising-like anisotropy while the d_z component favors an XY anisotropy. The smaller value of R_A for the bromide salts would indicate that the exchange anisotropies should favor stronger XY anisotropy in $(RNH_3)_2CuBr_4$ salts. This is in direct contrast to the magnetic anisotropy measurements. Thus, the exchange anisotropies must make a smaller contribution to the total magnetic anisotropy than the single-ion anisotropy.

Acknowledgment. The assistance of Dr. C. P. Landee with magnetic measurements and D. R. Bloomquist with crystallographic measurements is gratefully acknowledged. This work was supported by a grant from the NSF.

Registry No. II, 77460-74-3.

Supplementary Material Available: A listing of observed and calculated structure factors (2 pages). Ordering information is given on any current masthead page.

Contribution from Ames Laboratory—DOE[1] and the Department of Chemistry, Iowa State University, Ames, Iowa 50011

A Photoelectron Spectroscopic Study of the Zirconium Monohalide Hydrides and Zirconium Dihydride. Classification of Metal Hydrides as Conventional Compounds

JOHN D. CORBETT* and HENRY S. MAREK

Received December 28, 1982

Core and valence (Al Kα, He I) spectra are reported for $ZrH_{1.90}$ and for the layered $ZrXH_{0.5}$ and ZrXH (X = Cl, Br), in which hydrogen occurs in tetrahedral interstices between double metal layers. Significant Zr–H covalency is suggested by the valence XPS results for ZrXH and is very evident with $ZrH_{1.9}$, where a strong band appears at 4.8 eV. The very similar UV spectra for the chloride and bromide series show the development of a sharp hydride band at ~5.4 eV together with appreciable changes in the metal-rich band near E_F. A general consideration is provided of the interrelationships between the title compounds and binary metallic compounds formed by hydrogen and by other non-metals, halogen especially. These metal hydrides generally exhibit a consistent and well-defined pseudohalide-like anionic state with a binding energy 5–6 eV, a crystal radius of ~1.10 Å, and significant M–H covalency. Fluoride-like structures are appropriate for the hydrides on the basis of anion sizes, but isostructural pairs are found mainly with some tripositive metals because of the poor oxidizing power of H_2 and, possibly, the greater covalency of hydride. The behavior of hydrogen is regular in the sense that it appears to oxidize the metal in reduced compounds of other non-metals only to the same oxidation state that is achieved in the highest binary metal hydrides.

Introduction

Traditionally the metallic hydrides have been viewed as being somewhat separate and apart from the rest of chemistry, either with regard to the salt-like hydrides vs. halides, oxides, etc. or with respect to metal–metal-bonded and often metallic compounds containing other non-metals. Indeed, the metallic hydrides along with some other metal-rich compounds of the second-period non-metals have often been classified as "interstitial", a particularly inept term in many cases in view of the substantial structural and volume changes associated with their formation. Recent years have seen considerable gains in examples and understanding of metallic halides, chalcogenides, and pnictides and their interrelationships with both metals and "normal" (insulating or semiconducting) compounds. The chemistry of the metallic hydrides and their relationship to these other metallic phases have been pursued somewhat less intensively, and the time appears to be appropriate to consider whether a distinction in kind is really warranted. The properties of binary and ternary compounds of zirconium and neighboring elements with hydrogen, halide, and other non-metals are particularly instructive in establishing that the hydrides exhibit a plausible anion state with a set of properties nonlinearly related to the analogous halides.

The zirconium monohalides ZrCl and ZrBr[2] provide good representations of two-dimensional metals (including interstices) as they consist of four-layer slabs in which pairs of

(1) Operated for the U. S. Department of Energy by Iowa State University under Contract No. W-7405-Eng-82. This research was supported by the Office of Basic Energy Sciences, Materials Sciences Division.

(2) Struss, A. W.; Corbett, J. D. *Inorg. Chem.* **1970**, *9*, 1373.

0020-1669/83/1322-3194$01.50/0

close-packed zirconium layers are sheathed with pairs of close-packed chlorine layers.[3-5] Each metal atom in these is strongly bound to three neighbors in the other metal layer and somewhat less well to six in the same layer, for example at 3.09 and 3.43 Å, respectively, in ZrCl. This causes the interlayer metal polyhedra to be somewhat compressed relative to those in the hcp metal where the comparable distances are 3.18 and 3.23 Å. The zirconium monohalides are formally d^3, with three-fourths as many metal-bonding electrons as in the metal, and they attain a metal bond order that is 60% as great.

Both the bonding in ZrCl and ZrBr, which has been described theoretically,[6] and the metal-like reactions, which occur within these two-dimensional substrates, provide interesting comparisons with the behavior of the bulk metal. Thus, oxide may be continuously substituted in the (flattened) tetrahedral holes in ZrCl to a limit of 43 atom % (29 atom % in ZrBr),[7] comparable to the level of oxygen achieved in the octahedral interstices in the metal. (The choice of the polyhedron occupied in each case appears to depend principally on the attainment of typical Zr–O distances.) Reaction of the metal with more than a small amount of hydrogen gives a new phase ZrH_{2-x} (fluorite structure), while ZrCl and ZrBr each reversibly react with hydrogen between room temperature and ~450 °C to form first $ZrXH_{0.5}$ and, subsequently, the respective brass- or bronze-colored ZrXH.[8] All appear to be line phases at room temperature. The strength of the hydrogen–metal interactions in these compounds is about 70% of that in the metal hydride, judging from enthalpy data, and although the halohydrides are metastable with respect to Zr_6X_{12} and ZrH_2, the decomposition is significant only above ~600 °C.[9]

The first evidence regarding the disposition of hydrogen in the zirconium halohydrides came from NMR measurements that gave second moments consistent with hydrogen distributed principally in tetrahedral-like interstices.[10-12] Furthermore, the proton–proton interactions in a hemihydride phase reversibly related to the monohalide could be understood only with hydrogen present in zigzag chains of metal tetrahedra.[10] More recently, the heavy-atom structures for $ZrBrH_{0.5}$ and the isostructural ZrClH and ZrBrH have been solved from X-ray powder data to show that the incorporation of hydrogen is accompanied by a progressive lateral displacement of half of each slab with respect to the other, the first step indeed generating zigzag chains of distorted tetrahedra.[13] Incomplete neutron diffraction studies have qualitatively confirmed the correctness of the structural descriptions.

Photoemission spectra (XPS, UPS) of these compounds can provide useful information regarding the bonding states and their energy distribution. Earlier XPS and UPS studies[14] of the $ZrCl_x$ phases, $x = 1-4$, revealed that the valence bands at ~6 eV associated with what are mainly chlorine 3p valence levels are well separated from a nominal zirconium 4d band at ~1.2–2.0 eV. The zirconium 3d core levels show a 4.0-eV shift to higher binding energy on oxidation from the metal to $ZrCl_4$.[15] The present study of the halohydrides provides valuable information regarding the nature of the new hydrogen valence states obtained relative to those in ZrH_2 as well as evidence of the appreciable changes in "metal d" valence (conduction) states that occur on hydrogen incorporation in both the monohalides and the metal. In addition, these results, the nature of the reaction of hydrogen with other reduced phases, and the properties of metallic compounds that involve a variety of non-metals may be combined to provide some general insights and conclusions regarding the solid-state chemistry of the binary metal hydrides and their evident relationships to other classes of metal compounds.

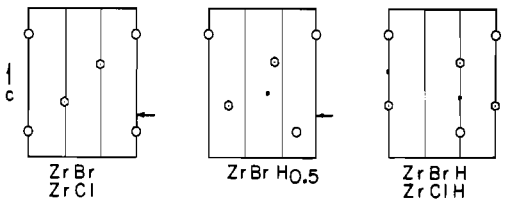

Figure 1. Schematic [110] representations of the intraslab relationships in ZrX, $ZrBrH_{0.5}$, and ZrXH (X = Cl, Br): ○, Cl or Br; ⊙, Zr; •, H. (For specific crystallographic relationships, see ref 13.)

Experimental Section

Materials. The preparation of the zirconium halide hydride phases studied has been described before.[13] Deuterides that had been prepared for vibrational studies were used as well as the hydrides. Reactor-grade Zr was allowed to react with 1 atm of H_2 at 550 °C until reaction ceased (2 days) to give a composition of about $ZrH_{1.90}$. All products were handled only in dryboxes, and their purities were verified by Guinier powder photographs.

The sample containers were opened in a helium-filled drybox (<1 ppm O_2, <0.5 ppm H_2O) attached directly to the sample port of the spectrometer. Each sample was pressed into a thin indium foil on the sample probe; the ability to so generate fresh surface and to cover the indium relatively well with these layered compounds contributed significantly to the quality of the data obtained. None showed any evidence of charging.

Spectral Measurements. Photoelectron emission spectra were obtained by using both X-ray (XPS, Al Kα, 1486.6 eV) and ultraviolet (UPS, He I, 21.21 eV) sources on an AEI Model ES-200B instrument coupled to a Nicolet 1180 minicomputer for data averaging and curve smoothing. Generally 2–11 and 20–300 scans were recorded in 512 channels with UV and X-ray sources, respectively, and the data were smoothed by 9- or 25-point running averages. A monochromator was used in the collection of the X-ray spectra reported for ZrClH and ZrH_2.

Many of the compounds studied gave UV spectra with very clear edges at the Fermi level, E_F, the location of which was highly reproducible. The instrument scale in the region of 3–8 eV also was checked against the fine structure for gold reported by Smith et al.[16] and was found to deviate from theirs by 0 to +0.2 eV. Any small changes in intensity within the spectra occasioned by changes in probe position were minimized by averaging data for several positions. The location of E_F in the XPS data was naturally less well-defined and sometimes not evident, and extrapolation from C 1s core levels produced from adventitious carbon was not sufficiently reproducible. However, the indium 4d peak was often sufficiently large to overwhelm the Cl 3s or Br 4s emission found in the same region, and so the unresolved In $4d_{5/2}$–$4d_{3/2}$ maximum was used as a reference after calibration with Au $4f_{7/2}$ emission from metal foil. With 84.0 eV for the latter,[17] an In 4d value of 17.0 eV was obtained, which compares with 17.2 (1) eV reported by Pollak et al.[18] The alternate use of a silver reference on the back of the sample probe used earlier[15] has

(3) Troyanov, S. I. *Vestn. Mosk. Univ., Ser. 2: Khim.* **1973**, *28*, 369.
(4) Adolphson, D. G.; Corbett, J. D. *Inorg. Chem.* **1976**, *15*, 1820.
(5) Daake, R. L.; Corbett, J. D. *Inorg. Chem.* **1977**, *16*, 2029.
(6) Marchiando, J. F.; Harmon, B. N.; Liu, S. H. *Physica B+C (Amsterdam)* **1980**, *99B+C*, 259.
(7) Seaverson, L. M.; Corbett, J. D. *Inorg. Chem.*, following paper in this issue.
(8) Struss, A. W.; Corbett, J. D. *Inorg. Chem.* **1977**, *16*, 360.
(9) Imoto, H.; Corbett, J. D.; Cisar, A. *Inorg. Chem.* **1981**, *20*, 145.
(10) Hwang, T. Y.; Torgeson, D. R.; Barnes, R. G. *Phys. Lett. A* **1978**, *66A*, 137.
(11) Murphy, P. D.; Gerstein, B. C. *J. Chem. Phys.* **1979**, *70*, 4552.
(12) Hwang, T. Y.; Schoenberger, R. J.; Torgeson, D. R.; Barnes, R. G. *Phys. Rev. B: Condens. Matter* **1983**, *27*, 27.
(13) Marek, H. S.; Corbett, J. D.; Daake, R. L. *J. Less-Common Met.* **1983**, *89*, 243.
(14) Corbett, J. D.; Anderegg, J. W. *Inorg. Chem.* **1980**, *19*, 3822.
(15) Cisar, A.; Corbett, J. D.; Daake, R. L. *Inorg. Chem.* **1979**, *18*, 836.
(16) Smith, N. V.; Wertheim, G. K.; Hufner, S.; Traum, M. M. *Phys. Rev. B: Solid State* **1974**, *10*, 3192.
(17) Bird, R. J.; Swift, P. *J. Electron Spectrosc. Relat. Phenom.* **1980**, *21*, 227.
(18) Pollak, R. A.; Kowalczyk, S.; Ley, L.; Shirley, D. A. *Phys. Rev. Lett.* **1972**, *99*, 275.

Table I. XPS Maxima (eV) for Zirconium Monohalide Hydrides and the Related Phases (Al Kα Source)[a]

	core		valence bands	
	Zr $3d_{5/2}$	X $(n-1)p^b$	X np	Zr
Zr[c]	178.5			0.8
$ZrH_{1.9}$	179.0		(H: 5.8)	0.7
ZrCl	179.4	199.6	6.8	1.6
$ZrClD_{0.5}$	179.7	199.7	6.7	1.2
ZrClH	179.6	199.7	6.5	1.0
$ZrCl_2$[d]	180.2	200.0		
ZrBr	179.5	189.9	6.0	1.6
$ZrBrH_{0.5}$	179.6	189.8	5.7	1.2
ZrBrH	179.6	189.7	5.6	0.9

[a] Core levels relative to C 1s = 285.0 eV. [b] $2p_{1/2}$ for Br owing to Br $3p_{3/2}$ overlap with Zr $3d_{3/2}$. [c] Reference 20. [d] Reference 15.

proven to be too sensitive to probe position.[19]

The hydrogen and metal band emissions observed for the monohalohydrides with He I radiation (only) were found to decrease significantly after some hours in the spectrometer ($P \sim 10^{-9}$ torr) or on long storage in the drybox. Since the extrapolated H_2 pressures are about 10^{-6} torr at room temperature,[8] a slow loss from the surface region of the sample was presumably occurring, and possibly oxidation of the surface as well. The use of a fresh sample and prompt measurement appeared to avoid this problem. The UPS (and XPS) data were otherwise reproducible and steady with time.

Results and Discussion

A comparison of the photoelectron emission characteristics of the zirconium monohalides and their hydrides is favored by their rather similar structures, all being composed of infinite four-layer slabs or sheets with quite similar distances between atoms. Figure 1 illustrates in terms of schematic [110] elevations how conversion of the monohalide to the hydride structures amounts to successive displacements of two of the layers in one slab with respect to the other half so that the close-packed ABCA layering in ZrBr (and ZrCl) transforms first to an intermediate packing in $ZrBrH_{0.5}$ and then to the ABAB ordering of the heavy atoms in ZrBrH (and ZrClH). ($ZrClH_{0.5}$ certainly has a closely related intraslab structure—as will be seen from the UPS results—but an apparently different stacking of these slabs.)

X-ray Spectra. Table I lists the relevant XPS data obtained for zirconium and halogen core energies as well as maxima for the two resolved valence bands of ZrX, $ZrXH_{0.5}$, ZrXH, and $ZrH_{1.9}$ while Figure 2 shows the valence spectra for ZrCl, $ZrClD_{0.5}$, and ZrClH. General experience has shown that a more or less regular increase in the binding energy of the metal core levels can be expected with increasing oxidation state, although such is marginally evident in the series ZrX–$ZrXH_{0.5}$–ZrXH. The progression ZrH_2 (179.0)–ZrClH (179.6)–$ZrCl_2$ (180.2 eV) probably reflects a normal and evidently more substantial change with electronegativity (covalence). Extraatomic screening of the core holes appears to be important in these phases when shifts are compared with those for higher chlorides.[21] The halogen core levels show the customary smaller changes.

The X-ray valence emission spectra all contain well-separated bands that can be tentatively assigned, as with ZrCl[6] and other reduced zirconium chlorides,[14] to predominantly halogen np states in the region 6–7 eV and a principally zirconium 4d emission near the Fermi level. Though this classification is not rigorous, the good separation of the narrow bands also points to limited mixing.[14,22] (The metal-rich band assignment is also supported by its greater than fourfold increase in relative intensity from ZrBr on change from 21.2- to 40.8-eV excitation.) Fairly constant ionization cross sections for these halogen and metal bands during hydride formation seem to be a reasonable assumption on the basis of what is found with the binary chlorides[14] while the photoemission cross section of hydrogen-like states to Al Kα radiation should be quite small.[23] In this case, simple models that have been developed for covalent bonding of a non-metal atom within metal polyhedra[24] might pertain, one electron per hydrogen coming from occupied zirconium valence states in the halide reactant with the metal orbital necessary to bind hydrogen coming either from the same zirconium valence states (as in $Nb_6I_{11}H$[25]) or from those lying above E_F in the reactant. However, the rigid-band model is well-known to be inapplicable to the periodic lattices of the metallic hydrides relative to the respective isostructural metal,[26] and it is clearly too simple in view of the XPS results (Figure 2).

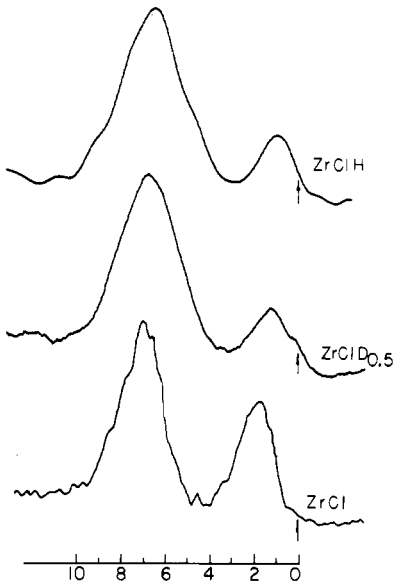

Figure 2. X-ray photoelectron emission results for the valence regions of ZrCl (unsmoothed, from ref 14), $ZrClD_{0.5}$, and ZrClH (Al Kα).

Even without these simplifications, the relative emission intensity from the two bands might be expected to change on oxidation by H_2 to reflect the loss of one electron per hydrogen from the zirconium 4d orbitals, the halogen np^6 emission remaining constant, provided there were no major changes in orbital mixing between the bands on incorporation of hydrogen. This circumstance does appear to apply to the XPS results for ZrCl, $ZrCl_2$, Zr_6Cl_{12}, and $ZrCl_3$, the ratios of the integrated intensity of the nominal Cl $3p^6$ emission to that for metal 4d increasing as expected (±10%) on oxidation of the metal from nominal d^3 (ZrCl) to d^1 ($ZrCl_3$) states.[14] For the hydride series this would mean that the ratio of X np:Zr 4d emission should increase as 6:3 to 6:2.5 to 6:2 or 1 to 1.2 to 1.5 on going from ZrX to $ZrXH_{0.5}$ to ZrXH. In fact, the apparent orbital distributions must not be so simple since the indicated ratio actually varies approximately as 1 to 1.9 to 2.1. The presence of substantial changes in the orbital populations of these bands on binding hydrogen was made clearer by subsequent UPS

(19) The locations of the Fermi energies in the UPS and XPS spectra of zirconium chlorides reported before[14] are all too low by ~0.4–0.8 eV. It also seems probable that the Cl 3p maxima generally do not occur at the same energy in XPS and UPS results (see text) and should not be used for cross-reference.

(20) Nguyen, T.-H.; Franzen, H.; Harmon, B. N. *J. Chem. Phys.* **1980**, *73*, 425.
(21) Corbett, J. D. *Inorg. Chem.* **1983**, *22*, 2669.
(22) Corbett, J. D. *Adv. Chem. Ser.* **1980**, *No. 186*, 329.
(23) Huang, J. T. J.; Rabalais, J. W. In "Electron Spectroscopy: Theory, Techniques and Applications"; Brundle, C. R., Baker, A. D., Eds.; Academic Press: New York, 1978; Vol. 2, p 253.
(24) Lauher, J. W. *J. Am. Chem. Soc.* **1978**, *100*, 5305.
(25) Nohl, H.; Andersen, O. K. *Conf. Ser.—Inst. Phys.* **1980**, *No. 55*, 61.
(26) Switendick, A. C. *Int. J. Quantum Chem.* **1971**, *5*, 459.

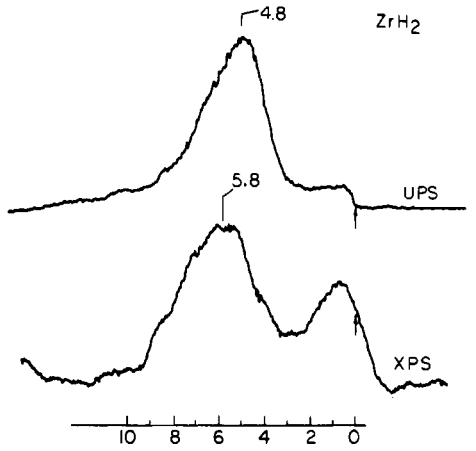

Figure 3. Valence spectra for $ZrH_{1.9}$ with UV (top) and X-ray (bottom) sources.

measurements, but some evidence for and understanding of this can be found in the simpler ZrH_{2-x} phase in which hydrogen occurs in metal tetrahedra (defect CaF_2 structure or a distorted variant thereof[27]) with substantially the same Zr–H distances as in the halide hydrides. In this case, the hcp metal substrate exhibits only a large density of states at E_F that falls off relatively smoothly with increasing binding energy.

Zirconium Dihydride. Figure 3 shows the UPS and XPS spectra for $ZrH_{1.9}$. The high cross section for hydrogen states expected[23,28] with the longer wavelength He I radiation is principally responsible for a large new band at 4.8 eV in the former. A smaller conduction band in which Zr 4d presumably predominates is also seen. Much more significant is the major new peak found near 5.8 eV in the XPS data, a striking reflection of the appreciable involvement of metal orbitals in covalent binding of hydrogen. Spectra with these characteristics have both been reported before but from somewhat different techniques and with different results. Weaver and co-workers[29] obtained a slightly more featured pattern with 21-eV synchrotron radiation (and a different collection mode). This contained a relatively larger metal band and a hydride band peaking at 5.3 eV with a clear shoulder or smaller peak at 7.2–7.8 eV depending on composition. No trace of the last feature, which they associated with tetragonal distortion in ZrH_{2-x} ($x < 0.35$ at room temperature), has been seen in the present work. The XPS spectrum of cubic $ZrH_{1.65}$ previously reported[30] was appreciably less well-defined owing to corrections necessary for its development, namely the subtraction of the ZrO_2 spectrum from that of an evidently comparable amount of the hydride using the intensities of either the separate zirconium 3d core levels for the two phases or the oxygen 2s peak. We saw no clear evidence of a ZrO_2 phase in the Zr 3d emission in any sample, and oxygen 2s could not be detected with $ZrH_{1.9}$. Peak positions were not reported for the derived $ZrH_{1.65}$ spectrum, but they appear to be at roughly 6.7 and 0.8 eV vs. 5.8 and 0.7 eV found here.

The non-self-consistent APW calculations for cubic ZrH_2 recently reported by Gupta[31] are nicely consistent with these observations. She showed that a considerable (though typical) number of $l = 2$ states occur within the zirconium sphere at

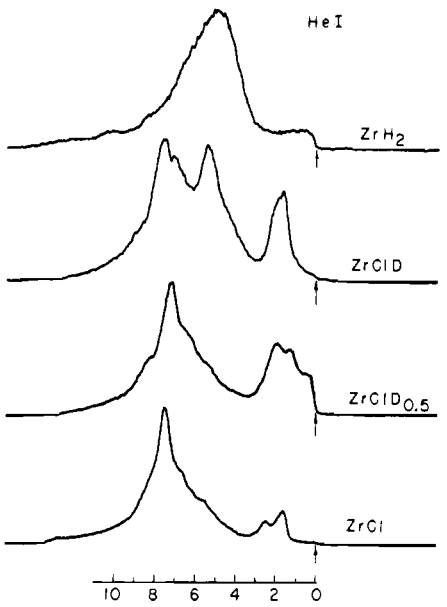

Figure 4. UPS spectra for ZrCl, $ZrClD_{0.5}$, ZrClD, and ZrH_2 (He I).

Table II. Ultraviolet Photoemission Maxima[a] (eV) for the Valence Region of Zirconium Monohalide Hydrides and Related Phases (He I)

	halogen *n*p	hydrogen	metal
Zr			0.3[b]
$ZrH_{1.9}$		4.8_5	0.9
ZrCl	7.4		1.6
$ZrClD_{0.5}$	7.1	(5.3)	1.9
ZrClD	7.5	5.4	1.6_5
ZrBr	6.7		1.6
$ZrBrH_{0.5}$	6.3	5.3	1.9
ZrBrH	6.6	5.5	1.5

[a] Not corrected for shifts caused by overlap. [b] Reference 14.

~6.5 eV below E_F together with the expected and similarly shaped distribution of $l = 0$ states within the hydrogen volume at the same energy, likewise indicating a significant Zr–H covalency in the nominal hydride valence band. The observed redistribution of metal d states (Figure 3) appears to be considerable if the X-ray emission data represent primarily a metal (high l) density of states, but of course some small hydrogen contribution is possible. The observation that these (mostly) metal d states in the anion valence band (by XPS) are ~1.0 eV more tightly bound than are hydrogen states (UPS) according to the maxima in Figure 3 is consistent with this and other calculations (e.g., Figure 3 in ref 32), the upper (lower binding energy) part of the so-called hydrogen band having more H–H antibonding and less Zr–H bonding character.

A general charge transfer from metal to hydrogen to give a well-bound and somewhat negative hydride state is clear from both band calculations and the valence and core photoelectron spectra of many metal hydrides (for example, ref 26, 29, and 31–34). A significant metal–hydrogen covalence is a general feature of theoretical studies, and evidence for this can also be seen in X-ray emission results, as for ZrH_2. Most significantly, the XPS data of Franzen et al.[35] for the alkaline-

(27) The tetragonal distortion of group 4 dihydrides as H:M approaches 2.0:1 is believed to be electronically driven and associated with an otherwise high density of states at E_F.
(28) Eastman, D. E. In "Electron Spectroscopy"; D. A. Shirley, Ed.; North-Holland Publishing Co.: Amsterdam, 1972; p 487.
(29) Weaver, J. H.; Peterman, D. J.; Peterson, D. T.; Franciosi, A. *Phys. Rev. B: Condens. Matter* **1981**, *23*, 1692.
(30) Veal, B. W.; Lam, D. J.; Westlake, D. G. *Phys. Rev. B: Condens. Matter* **1979**, *19*, 2856.
(31) Gupta, M. *Met.-Hydrogen Syst., Proc. Miami Int. Symp., 1981* **1982**, 381; *Phys. Rev. B: Condens. Matter* **1982**, *25*, 1027.
(32) Misemer, D. K.; Harmon, B. N. *Phys. Rev. B: Condens. Matter* **1982**, *26*, 5634.
(33) Switendick, A. C. *J. Less-Common Met.* **1976**, *49*, 283.
(34) Peterman, D. J.; Harmon, B. N.; Marchiando, J.; Weaver, J. H. *Phys. Rev. B: Condens. Matter* **1979**, *19*, 4867.
(35) Franzen, H. F.; Merrick, J.; Umana, M.; Khan, A. S.; Peterson, D. T.; McCreary, J. R.; Thorn, R. J. *J. Electron Spectrosc. Relat. Phenom.* **1977**, *11*, 439.

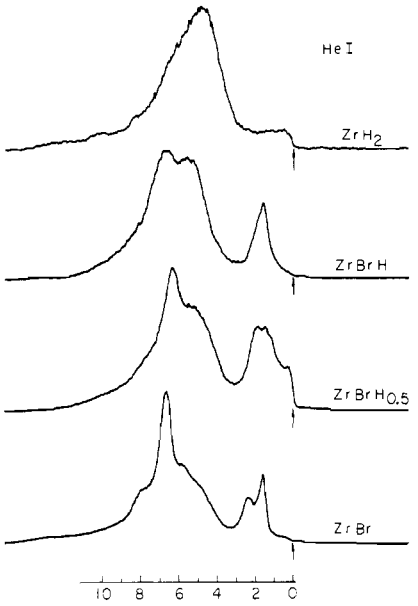

Figure 5. UPS spectra for ZrBr, $ZrBrH_{0.5}$, ZrBrH, and ZrH_2.

earth-metal dihydrides *also* show a substantial hydrogen band near 6.2 eV, again implicating the high cross section $(n-1)$d (and *n*p) metal orbitals in bonding. Of course, the metal conduction band is at this point empty. The electrons in a metal-based conduction band in YH_2, ZrH_2, NbH_2, etc. contribute to binding of the phases of course, but their presence appears to be a secondary feature since metal–hydrogen interactions apparently determine metal–metal separations in these high-symmetry structures. That these and other properties are not unique to hydrogen among the non-metals will also be considered later.

UV Spectra. With this background, the UPS results for the zirconium monohalide hydrides can be better understood. Spectra for the series ZrX–$ZrXH_{0.5}$–$ZrXH$–ZrH_2 are shown in Figures 4 and 5 for chloride[36] and bromide, respectively, while the numerical data for the emission maxima are listed in Table II.

The process of addition of hydrogen to tetrahedral interstices in ZrX together with the structural changes depicted in Figure 1 produces a regular and remarkable progression. The emission results are almost identical in the chloride and bromide series save for the expected (0.7-eV) displacement of the bromine *n*p level to a lower binding energy, giving strong evidence for the consistent purity of the samples studied. A substantial density of ionization states at E_F is seen to develop in $ZrClH_{0.5}$ with a band shape so like that in $ZrBrH_{0.5}$ as to encourage the conclusion that both must have very similar intraslab atomic and electronic structures and differ only in the stacking of these units. On further oxidation to the brass-colored ZrClH, this "metal" band sharpens and its centroid moves away from E_F. (E_F may have moved up as a gap developed, too, although on balance the UPS data for both ZrXH phases suggest they are metallic.) The two hydrogen additions are accompanied by the growth of a clear band at 5.3–5.5 eV though this feature in the hemihydride is really obvious only in the bromide. Association of the new peak with a characteristic hydrogen valence band quite analogous to that in ZrH_2 seems obvious.

Changes in all peak positions on oxidation (Table II) are very similar in both halide results as they also are in the XPS results (Table I). The small apparent changes in valence binding energies of halogen on oxidation could arise from movement of the E_F reference. The halogen *n*p peak appears to be at higher binding energy in UPS than in XPS data, suggesting the metal components arising from covalency may lie higher in the band as they appear less intense in UV data. (Compare relative intensities for ZrCl in Figures 2 and 4.) The width of the hydrogen band in ZrH_2 is determined largely by the dispersion of the upper of the two hydrogen bands of states, the energy of which reflects, among other things, H–H separations and antibonding interactions.[26,31] The single energy band for hydrogen in ZrXH must be relatively flatter and unperturbed by metal states, and likewise the metal by hydrogen, judging from the sharpness of the emissions; H–H separations in ZrClH (2.42 Å if these atoms are centered in the tetrahedra) are very comparable to those in cubic ZrH_2 but much fewer. Remember that the halogen is located on the outside of the double metal layers, well separated from the hydrogen, so that hydrogen–halogen antibonding repulsions in these compounds do not replace H–H interactions in the metal. Whether H–X effects might be communicated via the metal 4d orbitals is unknown, although a characteristic of these highly reduced halides, in contrast to sulfides, is that mixing of metal d and non-metal p valence orbitals is relatively small.[22] This is suggested by the ZrX spectra (Figures 4 and 5) and is confirmed by band theory.[6] The fact that hydrogen appears 0.5–0.7 eV more tightly bound in these mixed hydrides than in ZrH_2 may reflect the higher electron concentration achieved between the metal layers in ZrClH or just a higher relative position for the narrow metal d band and E_F.

In spite of the manifestly different structures, ZrH_2 and ZrXH appear to have a clearly similar bonding state for the hydrogen. Although the new hydrogen states are all filled by two electrons per atom, half of these coming from the (nonrigid) conduction band in Zr or ZrX, the result is not literally ionic, or even very close. Theory makes this clear for ZrH_2 as well as for hydrides of many neighboring elements, and this is beautifully evidenced by the strong component of this band in the X-ray emission data of ZrH_2. Halogen np^6 emission somewhat obscures this feature in the monohalide hydrides, but a shoulder at 4–5 eV, which presumably represents the metal 4d contribution to bonding hydrogen, is seen in the XPS data for ZrClH (Figure 2) and possibly in ZrBrH (not shown). The unusual enhancement of the XPS intensities in the region of the halogen band on oxidation of ZrX to $ZrXH_{0.5}$, which was noted earlier, is other evidence that a significant redistribution of metal 4d orbitals probably accompanies hydrogen binding.

A recurrent theme in the foregoing is that hydrogen in the hydrides studied has some characteristic and transferable properties, particularly an anion-like energy distribution of the valence electrons similar to what is found for many respectable anions (such as chloride[14]) in a variety of compounds. Nonetheless, one of the difficulties in achieving a general, even qualitative, appreciation and understanding of the seemingly unique role of hydrogen in the metal hydrides, especially as to their compositions, structures, bonding, and nonstoichiometries, has been a minimal appreciation of both their common chemistry as a group and the relationship between them and other compounds. But relatively recent experimental and theoretical investigations of hydrides together with like studies of new metallic and metal-rich phases of other non-metals now make such a consideration much more informative and practical. Within this context many hydrides appear unexceptional, with properties perfectly appropriate to compounds of such a small covalently bonded non-metal. The following will expand on this evidence and that conclusion.

Hydride Characteristics and Comparisons. The comparative examination of hydrides will take the directions outlined in Table III: the consideration of (1) valence electron distribu-

(36) The small cusp at E_F for ZrCl is highly reproducible and appears to mark the upturn in $N(E)$ at that point predicted by band theory.[6]

Table III. Characteristic Properties of the Hydride Anion

characteristics	comparisons
well-bound anion state 5–6 eV below E_F, often with secondary M–M bonding	valence electron distributions in metallic hydrides very comparable to those with other non-metals, e.g., LaS, NbO, and ZrCl
significant covalency; metal d orbitals appreciably involved in bonding hydride	comparable covalency found with many other non-metals, fluoride excepted
reproducible size with a crystal radius of 1.10 Å when normal-valent radii are utilized for the metals; predictable structure types found in most cases	closest comparison with fluoride (r(IV) = 1.17 Å); conduction electrons not screening to M–H interactions
produced by a poor oxidizing agent (H_2), often yielding metal in low oxidation state in a metallic compound	few comparisons occurring with fluorides since F_2 is a good oxidizing agent (YF_2, ZrF_2, NbF_2 unknown)
consistent oxidation state of −1, binary and ternary hydrides of a given metal exhibiting the same limiting oxidation state for the metal	ZrH_2 vs. ZrClH; LaI_2H vs. LaH_2; $TiOH_0$ vs. TiH_2[a]

[a] More examples in a later table.

tion, (2) covalency, (3) size and structure, (4) H_2 as an oxidizing agent, and (5) regularities in metal oxidation states achieved. The rather obvious consideration of hydride as a pseudohalide is of course not new, but earlier considerations[37-39] did not have available the rather compelling evidence provided by photoelectron spectra and band theory as well as much of the knowledge on analogous metallic compounds of other non-metals and on some chemical regularities of hydrides. In fact, clear and direct analogies between hydrides and halides turn out to be sufficiently small as to require further comment.

Valence Bands. A considerable amount of PES data in the literature (e.g., ref 29, 34, 35, and 40) as well as Figures 3–5 demonstrates that hydride exhibits a "fingerprint" characteristic of a filled valence band 5–6 eV below E_F, at least in hydrides of metals of the first five groups. This in itself is informative but not at all unusual; a great variety of reduced compounds are now known that exhibit some combination of ionic and covalent and metallic (or metal–metal) bonding, a metal band at or near E_F and a filled valence band originating mainly with the non-metal that lies some 5–7 eV below the Fermi level. Metal valence electrons that are not utilized in filling non-metal valence orbitals remain involved in metal–metal bonding, in contrast to the behavior of many 3d compounds (e.g., VCl_2, $Fe(NO_3)_2$, and NiO). Binding of the non-metal naturally always includes some degree of covalent interaction with the metal, the latter amounting to a mixing of valence orbitals between the non-metal-based (valence) and metal-based (conduction or metal valence) bands, including metal states that otherwise lie above E_F. The amount of this is apparently greatest for carbides, nitrides, etc., appreciable for sulfides, phosphides, and iodides, and less for chlorides, oxides, and the very few fluorides known to exhibit significant metal–metal bonding. The metal–metal bonding may appear structurally dominant or secondary.

Some of the more familiar examples of metallic salts are found in the rock-salt structure, ScS, TiO, VO, $Zr_{1-x}S$, and NbC, and the monosulfides of most of the rare-earth metals, but they are also recognized in the unique NbO, NbO_2, and Ti_2N (TiO_2 type), TiS and VS (NiAs), and many lower symmetry examples such as TiP, NbS, Ta_2P, and Nb_5Se_4.[41] Band structure calculations and XPS data available particularly for higher symmetry examples and ZrCl support the generalization in the previous paragraph regarding the redistribution of the valence electrons of the component atoms into conduction and filled valence bands.[6,20,42-45] Non-metals

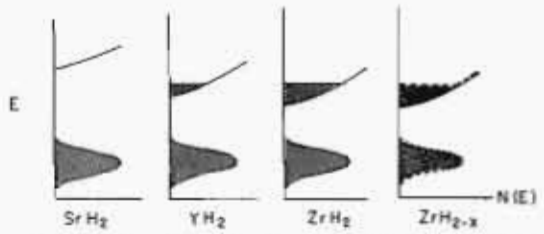

Figure 6. Schematic valence density of state diagrams for SrH_2, YH_2, ZrH_2, and ZrH_{2-x} (see text).

with oxidation states of −2 or −3 are common among these, a factor which allows more frequent approach of the metal atoms and an increased mixing of the non-metal and conduction bands.

Uninegative (halide) examples with which one might compare (or contrast) the metallic hydrides were until recent years limited to Ag_2F (inverse CdI_2 type). Many more examples are now known, but usually with a significantly lower dimensionality as in the ZrX phases (which also occur for many of the rare-earth elements), the layered LaI_2 ($MoSi_2$), and chain structures Y_2Cl_3, Sc_5Cl_8, and so forth.[46,47] At least the chlorides appear to involve less mixing of halide and metal and therefore exhibit sharper PES bands and lower dimensionality in the M–M interactions than do the heavier chalcogenides and iodides.[22] Strong metal–metal interactions may also give rise to splitting of the d manifold and semiconduction in sheets (MoS_2, $ZrCl_2$[15]) or chains (Gd_2Cl_3,[48] ZrI_2[49]). A larger number of anions or their larger size relative to the metal-based orbital radii may be responsible for the lower dimensionality of the M–M interactions in some of these and even more localized examples as clusters, Zr_6X_{12}, Mo_6S_8, etc.[50]

The close interrelationships in valence electron distribution between metallic hydrides and other metallic compounds in higher symmetry structures lead to the following conclusion: The metallic hydride compounds, at least those of the groups 3–5, lanthanide and actinide elements, should as a group be considered relatively normal metallic salts with structures appropriate to that particular non-metal. Also, the hydrides differ from the normal-valent ("saline") KH, CaH_2, LaH_3, etc. not in kind but principally in the occupation of a conduction band associated largely with the metal cores and from metallic

(37) Gibb, T. R. P. *Prog. Inorg. Chem.* **1962**, *3*, 315.
(38) Libowitz, G. G. "The Solid State Chemistry of Binary Metal Hydrides"; W. A. Benjamin: New York, 1965.
(39) Messer, C. E. *J. Solid State Chem.* **1970**, *2*, 144.
(40) Weaver, J. H.; Peterman, D. J.; Peterson, D. T. *NATO Conf. Ser., Ser. 6* **1983**, 207.
(41) Franzen, H. F. *Prog. Solid State Chem.*, **1978**, *12*, 1.
(42) Ihara, H.; Hirabayashi, M.; Nakagawa, H. *Phys. Rev. B: Solid State* **1976**, *14*, 1707.
(43) Schwarz, K. *J. Phys. C* **1977**, *10*, 195.
(44) Neckel, A. *Int. J. Quantum Chem.* **1983**, *23*, 1317.
(45) Nakahara, J.; Franzen, H.; Misemer, D. K. *J. Chem. Phys.* **1982**, *76*, 4080.
(46) Corbett, J. D. *Acc. Chem. Res.* **1981**, *14*, 239.
(47) Simon, A. *Angew. Chem., Int. Ed. Engl.* **1981**, *20*, 1.
(48) Ebbinghaus, G.; Simon, A.; Griffith, A. Z. *Naturforsch., A* **1982**, *37A*, 564.
(49) Guthrie, D. H.; Corbett, J. D. *J. Solid State Chem.* **1981**, *37*, 256.
(50) Corbett, J. D. *J. Solid State Chem.* **1981**, *37*, 335.

compounds of other non-metals chiefly because of the rather distinctive combination of size and bonding characteristics of hydrogen and their consequence on the observed structure type and properties. The familiar distribution of valence electrons depicted in Figure 6 for the SrH_2–YH_2–ZrH_2 series within a rigid-band approximation could just as well pertain to the analogous sulfides, nitrides, etc. or the hypothetical difluorides. However, certain factors that do not all pertain to compounds of other non-metals, halide especially, must be recognized since it is these that make hydrides appear somewhat distinctive, viz., the particular polarizability and size of hydride and the oxidizing power of hydrogen.

Covalency. A fact that was not always appreciated in earlier considerations of solid-state hydride chemistry was the greater polarizability of the valence shell of H^-, the binding (and density) of two electrons therein being much less than the six valence electrons in fluoride. The resultant covalency is evident from both band calculations and X-ray photoelectron data (Figure 3). Covalency and an inability to include metal–metal bonding in a meaningful way where necessary were doubtlessly significant in the deficiencies of earlier Born–Haber type calculations of hydride stability.[37]

Anion Size. The concept of a reasonable and reproducible anionic behavior for hydrogen is indicated not only by the existence of a well-defined valence-state population and energy but also by a quite consistent volume or radius requirement in the same metal hydrides. (Again, the "anionic" appellation should *not* be equated with "ionic".) Reaction of hydrogen with transition metals gives first a usually small solid solution region (where hydrogen often occupies tetrahedral holes[51]) and then a new phase, for example YH_2, LaH_2, TiH_2, ZrH_2, or ThH_2 (often substoichiometric) in a normal or tetragonally distorted[27] fluorite structure or other types such as NiH_{1-x} and PdH_{1-x} (NaCl), NbH, or UH_3, and further reaction yields such phases as NbH_2 (CaF_2), Th_4H_{15}, and MH_{3-x} for most of the rare-earth elements.[38,52] Noteworthy in these processes is a substantial volume increase, which as noted early on by Rundle and co-workers,[53] greatly lessens the metal–metal bonding and replaces it by metal–hydrogen bonding. (Only the more weakly bound alkali and alkaline-earth metals involve a volume decrease on hydride formation.) Metal–metal separations in high-symmetry structures such as the NaCl and CaF_2 types appear to be determined almost entirely by characteristic metal–non-metal distances,[54] one example of matrix effects.[50,55]

Interestingly, Libowitz[38] noted some years ago that the M–H distances in 27 hydrides of transition groups 3–5, lanthanide and actinide elements were well reproduced (0.03 Å average deviation) by sums of *normal-valent* cation radii, i.e., for Zr^{4+}, La^{3+}, and Nb^{5+}, together with a fixed 1.27-Å radius for H^-. The use of more recent *crystal* radii[56] for the metals fit the collection equally well with 1.10 Å for H^-, remembering that the superscript describes an oxidation state not a charge. It is pleasing to note that NiH_{1-x}, PdH_{1-x} (NaCl), and CrH (*anti*-NiAs) are also so described.[57] The earlier list included only two non-metallic hydrides, EuH_2 and YbH_2, but distances in several more examples from subsequent studies, MgD_2,[58] CaD_2,[59] and $LiMX_3$ (M = Sr, Ba, Eu, inverse perovskite),[60–62] fit equally well.[63] There appears to be no distinction in the distance property as to whether the phase is metallic or not. The absence of substantial screening between the (normal-valent) metal core and the non-metal is also a feature of many other metal-rich and metal–metal-bonded compounds[38,46] as long as one avoids classical examples such as nonconducting compounds of the 3d elements where the differentiating electron is localized on the cation. The absence of metal–non-metal screening by the delocalized electrons seems particularly reasonable in segregated structures such as ZrCl (Figure 1) since the chlorine atoms are on the outside of the double metal layers between which the metal–metal bonding is effective. However the directional differentiation between Zr–Zr and Zr–S bonding about the metal in ZrS (NaCl) is also clearly seen in what are t_{2g} and e_g orbital sets at the zone center.[20] The same is found in LaH_2 and LaH_3.[32]

Many observed hydride crystal structures are quite reasonable for an anion with a crystal radius of ~1.10 Å when these are compared with those for fluoride with a four-coordinate radius of 1.17 Å.[56] The fluorite structure known for many dihydrides, SrF_2 etc., would undoubtedly also apply to the hypothetical YF_2, ZrF_2, NbF_2, etc. As noted before by Messer,[39] a striking structural correspondence is found between the (semiconducting) trihydrides and known trifluorides. The so-called HoD_3 structure type found for the MH_3 phases where M = Y, Sm–Lu, and Np–Am is better known as the trigonal tysonite (LaF_3) structure and occurs in the trifluorides La–Ho, Ac, and U–Cm.[64] The range of metals found with each non-metal is very appropriate to a slightly greater radius for fluoride. On the basis of size alone, the cubic structure found for MH_3 where M = La–Nd (*anti*-Li_3Bi—fluorite plus hydrogen in all octahedral interstices[65]) might be expected for trifluorides of the early actinides, but perhaps covalency is of some significant consequence in MH_3.

A covalent effect may be responsible for the alkaline-earth-metal dihydrides adopting the $PbCl_2$ (rather than the CaF_2) type structure, which is also exhibited by the alkaline-earth-metal difluorides under pressure.[66] Although structures of the likes of UH_3 and Th_4H_{15} seem strange by comparison, the lack may be in examples and understanding of analogous metal-rich compounds involving other non-metals. As we have seen, the size of hydride requires smaller interstices and thus frequently occurs in metallic phases where relatively good metal–metal bonding can still be retained in three dimensions. In comparison, most larger anions (Cl, S) are considerably more limiting to metal–metal approach, particularly at comparable non-metal:metal ratios. Oxide has some small similarities with hydride in metallic phases such as TiO, NbO, α-ZrO_x, β-VO_2, and TaO_2.

(51) Khatamian, D.; Stassis, C.; Beaudry, B. J. *Phys. Rev. B: Condens. Matter* **1981**, *23*, 624.
(52) Mueller, W. M.; Blackledge, J. P.; Libowitz, G. G. "Metal Hydrides"; Academic Press: New York, 1968.
(53) Rundle, R. E.; Shull, C. G.; Wollan, E. O. *Acta Crystallogr.* **1952**, *5*, 22.
(54) Rundle, R. E. *Acta Crystallogr.* **1948**, *1*, 180.
(55) Matrix effects limit M–M bonding whenever (a) the anion size is sufficient that anion–anion contacts restrict M–M approach for small M, as in M_6X_{12}-type clusters, or (b) the metal–non-metal distances in a high-symmetry structure determine M–M separations, as in NaCl and CaF_2 types.
(56) Shannon, R. D. *Acta Crystallogr., Sect. A* **1976**, *32A*, 751.
(57) These three give $r(H) \sim 1.04$ Å with six-coordinate radii for Ni^{2+}, Pd^{2+}, and Cr^{2+} (low spin). Some covalent shortening might be expected with these and seems clear for CuH (wurtzite structure) with a calculated value of 0.99 Å.
(58) Zachariasen, W. H.; Holley, C. E., Jr.; Stamper, J. F., Jr. *Acta Crystallogr.* **1963**, *16*, 352.
(59) Andresen, A. F.; Maeland, A. J.; Slotfeldt-Ellingsen, D. *J. Solid State Chem.* **1977**, *20*, 93.
(60) Messer, C. E.; Eastman, J. C.; Mers, R. G.; Maeland, A. J. *Inorg. Chem.* **1964**, *3*, 776.
(61) Messer, C. E.; Hardcastle, K. *Inorg. Chem.* **1964**, *3*, 1327.
(62) Maeland, A. J.; Andresen, A. F. *J. Chem. Phys.* **1968**, *48*, 4660.
(63) A reasonable radius may pertain to α-phase systems as well; $YD_{0.176}$ (hcp) is close to saturation ($YD_{\sim 0.19}$), and the tetrahedral interstices therein,[51] which are less than 10% occupied, are essentially the same size as found in $YD_{1.96}$ (distorted CaF_2), with which it is (nearly) in equilibrium, viz., d(Y–D) = 2.22 (average) and 2.25 Å, respectively.
(64) Wells, A. F. "Structural Inorganic Chemistry", 4th ed.; Clarendon Press: Oxford, England, 1975; pp 295, 357.
(65) The cubic structure was formerly described as BiF_3 type, but the latter phase is actually an oxyfluoride with a defect version of the *anti*-Li_3Bi structure.[64]
(66) Seifert, K.-F. *Ber. Bunsenges. Phys. Chem.* **1966**, *70*, 1041.

Table IV. Products of the Reversible Reaction of Hydrogen with Reduced Compounds

substrate	max hydride[a]	formal oxidn state	hydride limit[b]
	Reaction		
ZrCl, ZrBr	$ZrXH_{1.0}$	+2	ZrH_2
Nb_6I_{11}	$Nb_6I_{11}H$	+2	NbH_2
$CsNb_6I_{11}$	$CsNb_6I_{11}H$	+1.83[c]	
LaI_2, NdI_2	MI_2H[d]	+3	$(La, Nd)H_3$
ThI_2	$ThI_2H_{1.77(5)}$[d]	+3.77 (5)	$ThH_{3.75}$
	No Reaction		
SmI_2	none	+2	SmH_2
TiO	none	+2	TiH_2
$TiCl_2$, TiI_2	none (<0.1 H)	+2	
$ZrCl_3$	none (<0.1)	+3	ZrH_2
Zr_6Cl_{12}	none (<0.02)	+2	
Nb_6Cl_{14}	none (<0.01)	+2.33	$(Nb, Ta)H_2$
Ta_6Cl_{15}	none (<0.05)	+2.5	
$Na_4[(Ta, Nb)_6Cl_{12}]Cl_6$	none (≤0.1)	+2.33	
Mo_6Cl_{12}	none (0.06)	+2	MoH_0
Mo_6S_8	none	+2.67	
Pd_3P	none[e]	+1	PdH
	Decomposition		
$NdCl_2$			
Y_2Cl_3[f]			
LaCl[f]			

[a] As achieved with ~1-2 atm H_2; ref 8, 9, 67, 69, 70. [b] Reference 38; neglecting small nonstoichiometries. [c] H uptake is presumably limited by available interstices. [d] Unknown structure. [e] Rundqvist, private communication, 1981. [f] Marek, H. S.; Corbett, J. D., unpublished research.

Oxidizing Power. The relatively limited correspondence between hydrides and fluoride originates with the great differences in oxidizing power of the elements H_2 and F_2. The low oxidizing capability of H_2 is illustrated by the fact that it converts Y, Zr, and Nb only to the dihydrides, leaving one-third, one-half, and three-fifths of the metal electrons retained in (weakened) metal–metal bonding. Although the corresponding fluorides YF_2, ZrF_2, and NbF_2 should be very similar, they remain hypothetical because the higher oxidizing power of F_2 leads to relatively more stable YF_3, ZrF_4, etc. and hence to disproportionation of the difluorides. Thus, the structural correspondence between hydrides and fluorides is limited to a relatively few cases where the former achieve fairly normal oxidation states. The increase in radius between the second- and third-period nonmetals is relatively large, and so the change from fluoride to chloride where comparably low oxidation states are stable yields a new and different structural chemistry. One is left with some compounds for which a halide (or other) analogue cannot be imagined, for example, the complex lower hydrides (H/M < 1) formed by the bcc metals of group 5 where a fascinating and perhaps unique chemistry occurs within the parent metal phase.

Limiting Oxidation States. An assignment of a formal −1 oxidation state to hydride in accord with full occupancy of the hydrogen valence band seems fully as meaningful as in compounds of other non-metals. A particularly remarkable verification of the regular character of hydrogen in hydrides is the observation by Imoto[67] that a reduced halide, oxide, etc. apparently will absorb hydrogen only if the metal oxidation state therein is less than that in the highest binary hydride of the same metal and, furthermore, that the amount of hydrogen absorbed will produce an oxidation state for the metal no higher than that in the binary hydride.[68] The available data to this point are summarized in Table IV. Thus, one finds comparable pairs ZrXH vs. ZrH_2, LaI_2H vs. LaH_3, $Nb_6I_{11}H$ vs. NbI_2, and (too-good-to-be-true) $ThI_2H_{1.77}$ vs. $ThH_{3.75}$. On the other hand, phases such as $MoCl_2$, TiO, TiI_2, Zr_6Cl_{12}, and Nb_6Cl_{14} are as oxidized as or more oxidized than the respective binary hydride and none takes up hydrogen. However, finer details of halide hydride stability relative to the metal hydrides, which are reflected in measured ΔH and $P(H_2)$ values (e.g., LaI_2H vs. LaH_3[70]), are not understood, and their presence may yet cause some deviations in composition from the metal hydride references.

The apparent equivalence of halogen and hydrogen with respect to oxidation of a given metal, which is implied by the limited number of examples in Table IV, may also be a matter of some luck. One can imagine binary metal hydrides that are unstable because the H–H separations are too short (antibonding effects) but that may be perfectly stable in that metal oxidation state in a ternary hydride when the H–H interactions are reduced in the new structure. A good example may be with scandium, where the relatively short Sc–H distance in either the LaF_3 or the *anti*-Li_3Bi type structure for the unknown ScH_3 would fix the hydrogen separations at much too small a value. The instability of ScH_3, TiH_3, MoH_2, etc., corresponding to H bands crossing E_F, has been treated in terms of empirical energy band parameters by Switendick.[26] The results of several reactions of hydrogen with reduced scandium halides[69] suggest the product *may* have an oxidation state above +2, but this is uncertain until the unknown product is shown to be single phase and the possibility of impurities eliminated. The effects of alloy or intermetallic formation on hydrogen reactivity of a given element appear more complex and not easily related to simple ideas developed in Table IV.

Finally, it might be noted that the occurrence of nonstoichiometry in the metallic hydrides (and in many other metallic compounds) in high-symmetry structures is relatively common and easy to understand (or rationalize). A depiction of this for $ZrH_2 \rightarrow ZrH_{2-x} + (x/2)H_2$ is given in Figure 6, where loss (or gain) of x atoms from tetrahedral sites causes a disappearance (or increase) of a like number of states from the hydrogen band and a corresponding change in the electron concentration in the conduction band. (The former change is represented to take place in a symmetric manner in the figure, but the disappearing states presumably come largely from the upper (antibonding) region of the band.) At least some of the metal contribution to covalent bonding of the hydrogen lost will now appear as low-lying states in the conduction band, broadening the band and providing some driving force in lowering E_F. (The lattice constant also decreases.) Switendick has deduced that this sort of change in E_F applies to TiH_{2-x}.[33] Conversely, the addition of hydrogen to a substoichiometric hydride is well understood to raise E_F; although one electron per hydrogen is removed from the conduction band, so are some metal d states for covalent bonding that formerly contained two electrons each. There have been many comparisons of the energy band distribution in a hydride relative to that in the expanded metal with the same (sometimes hypothetical) structure in terms of changes in E_F and what this means in classification and metal hydride models.[26,33] However, this may be somewhat misleading; from a chemical viewpoint, exactly the same considerations pertain qualitatively because of the obvious covalent bonding when other non-metals react with metals to form metallic compounds, e.g., Ag_2F, ZrBr, and TiS from the corresponding metal lattice. Certainly there would be no good reason for an analogous consideration in these cases whether a positive or a negative model for the

(67) Imoto, H.; Corbett, J. D. *Inorg. Chem.* **1980**, *19*, 1241.

(68) The earlier suggestion[69] that delocalized electrons were necessary (but not sufficient) for hydrogen uptake appears to be coincidental but is still an appropriate circumstance for the low oxidation state halides involved.

(69) Struss, A. W.; Corbett, J. D. *Inorg. Chem.* **1978**, *17*, 965.

(70) Imoto, H.; Corbett, J. D. *Inorg. Chem.* **1981**, *20*, 630.

non-metal was indicated by an increase or decrease in E_F on their formation.

Acknowledgment. The authors are indebted to J. W. Anderegg for the high-quality photoelectron spectra and to H. F. Franzen and B. N. Harmon for helpful and informative discussions.

Registry No. ZrCl, 14989-34-5; $ZrClD_{0.5}$, 87206-68-6; ZrClH, 60921-39-3; ZrBr, 31483-18-8; $ZrBrH_{0.5}$, 60967-29-5; ZrBrH, 60921-40-6.

Contribution from Ames Laboratory—DOE[1] and the Department of Chemistry, Iowa State University, Ames, Iowa 50011

Synthesis and Characterization of Oxide Interstitial Derivatives of Zirconium Monochloride and Monobromide

LINDA M. SEAVERSON and JOHN D. CORBETT*

Received February 14, 1983

The reactions of ZrO_2 with double-metal-layered ZrCl and ZrBr at ~980 °C and with Zr metal at 930 °C have been studied with the aid of high-resolution (Guinier) powder pattern data. The products of the first reaction are $ZrX(O_y)$, an expanded ZrX structure, and $Zr(O_x)$ from solution of ZrO_2 in the metal, viz., $ZrX + nZrO_2 = ZrX(O_y) + nZr(O_x)$. The oxygen composition of both products (y, x) varies continuously up to the point of ZrO_2 saturation where n, y, and x are respectively 0.27 (1), 0.43 (2), and 0.42 for chloride and 0.22 (2), ~0.35, and ~0.42 for bromide. Single-crystal X-ray results for $ZrBrO_{\sim 0.23}$, $ZrClO_{0.29}$, and $ZrClO_{0.43}$ establish the retention of the basic ZrX structure ($R\bar{3}m$) and the concentration of oxygen, which is distributed randomly in the distorted tetrahedral interstices between the zirconium layers. The last named composition (a = 3.4984 (2) Å, c = 27.065 (4) Å) is in equilibrium with ZrO_2 and gave a refined structure with R = 0.046 and R_w = 0.056 for 141 independent reflections with $2\theta \leq 59.9°$. UPS measurements show that the chloride oxide is still metallic. Attempts to achieve analogous products from reactions between ZrCl and ZrC, ZrN, ZrF_4, or $Zr_{1+x}S$ and diverse attempts to intercalate ZrCl were unsuccessful. The mean Zr–O distance in $ZrClO_{0.43}$, 2.07 Å, is close to that found in tetragonal and monoclinic ZrO_2 and to the sum of conventional crystal radii, in agreement with the general observation that significant screening is not provided by the delocalized electrons. The size of the available interstices in ZrX and the metal appear to be important factors in oxide substitution in the T_d and O_h sites, respectively, and in the course of the other ZrX reactions studied. Fluoride substitution evidently fails because of the absence of an analogous $Zr(F_x)$ metal product.

Introduction

The novel structures of the zirconium monohalides ZrCl and ZrBr provide a basically two-dimensional metal-like substrate for study. These phases consist of cubic-close-packed layers of zirconium and halide atoms stacked in pairs to yield the sequence X–Zr–Zr–X[2-4] with relative orientations AbcA. These tightly bound four-layer slabs are in turn weakly bound in the order ABCA (designating outer halogen layers only) in ZrCl or ACBA in ZrBr. The strength of the metal–metal interactions are revealed by the short metal–metal distances, for example, three at 3.09 Å in the other layer and six at 3.43 Å in the same layer in ZrCl vs. comparable distances of 3.18 Å and 3.23 Å in the hcp metal. The d orbitals are strongly split by these interactions, but the materials are still metallic[4-7] and graphite-like[8] and are therefore candidates for interesting reactions and products. Thus, both substrates take up hydrogen with small changes in layering to form $ZrXH_{0.5}$ and ZrXH in which hydrogen is in tetrahedral interstices as it is in ZrH_{2-x} (defect fluorite structure).[9-11] Other studies of the monohalides include their use as synthetic intermediates[12,13] and unsuccessful attempts at intercalation with metal ions.[4] One particularly interesting observation by Daake[14] was that the lattice constants of ZrCl and ZrBr increase 1–2% on reaction with ZrO_2 at 850 °C. The change was suggested to arise from loss of electron density between the zirconium layers accompanying the substitution of oxide in the halide layers, viz., $ZrX_{1-n}O_n$.

The present article reports an investigation of these ZrX–ZrO_2 reactions and products, especially the identification of the reaction stoichiometry and the structure and photoelectron spectra of the oxidized ZrX phase. Analogous reactions of other non-metals with ZrX and further attempts to intercalate ZrCl are also described.

Experimental Section

Syntheses. The moderate air and moisture sensitivity of the reactants and products even at room temperature dictates the use of typical drybox and vacuum techniques. The dryboxes were constantly purged with dry N_2 that recirculated through a column of molecular

(1) Operated for the U.S. Department of Energy by Iowa State University under Contract No. W-7405-Eng-82. This research was supported by the Office of Basic Energy Sciences, Materials Sciences Division.
(2) Troyanov, S. I. *Moscow Univ. Chem. Bull. (Engl. Transl.)* **1973**, *28*, 89.
(3) Adolphson, D. G.; Corbett, J. D. *Inorg. Chem.* **1976**, *15*, 1820.
(4) Daake, R. L.; Corbett, J. D. *Inorg. Chem.* **1977**, *16*, 2029.
(5) Troyanov, S. I.; Tsirel'nikov, V. I. *Russ. J. Inorg. Chem. (Engl. Transl.)* **1970**, *15*, 1762.
(6) Marchiando, J. F.; Harmon, B. N.; Liu, S. H. *Physica B+C (Amsterdam)* **1980**, *99B+C*, 259.
(7) Corbett, J. D.; Anderegg, J. W. *Inorg. Chem.* **1980**, *19*, 3822.
(8) Dean, R. S. *Ind. Lab.* **1959**, *10*, 45.
(9) Struss, A. W.; Corbett, J. D. *Inorg. Chem.* **1977**, *16*, 360.
(10) Marek, H. S.; Corbett, J. D.; Daake, R. L. *J. Less-Common Met.* **1983**, *89*, 243.
(11) Corbett, J. D.; Marek, H. S. *Inorg. Chem.*, preceding paper in this issue.
(12) Daake, R. L.; Corbett, J. D. *Inorg. Chem.* **1978**, *17*, 1192.
(13) Cisar, A. J.; Corbett, J. D.; Daake, R. L. *Inorg. Chem.* **1979**, *18*, 836.
(14) Daake, R. L. Ph.D. Dissertation, Iowa State University, 1976.

0020-1669/83/1322-3202$01.50/0